Low Cost Artificial Planar Target Measurement Techniques for Terrestrial Laser Scanning

Jacky CHOW, Axel EBELING, and Bill TESKEY, Canada

Key words: Laser scanning, signalized targets, quality assessment, least-squares, geometric form fitting

SUMMARY

This paper presents both an internal and external accuracy assessment of four different methods for measuring the centroid of a signalized planar target captured by a terrestrial laser scanner. The planar targets used in this project are composed of a black background and a white circle printed on 8½ by 11 inches plain sheet of paper using a consumer level LaserJet printer. The first two methods tested define the centroid of a target to be the mean and median of the cluster of points belonging to the white circle in the point cloud. The latter two methods are more advanced, and they take advantage of the planar nature of the target as well as the intensity difference between the circle and the background to strengthen the centroid derivation through a combination of least-squares plane fitting and circle fitting. The main benefit of the four presented methodologies is that no specialized and/or laser scanner dependent targets need to be utilized. And it will be demonstrated in this paper that using the two advanced methods can yield position measurement precision and accuracy far superior to the simple mean or median computations. In fact, sub-millimetre precision and accuracy is achievable from using low cost paper targets provided that an appropriate target measurement algorithm like the latter two methodologies proposed in this paper is adopted.

Low Cost Artificial Planar Target Measurement Techniques For Terrestrial Laser Scanning

Jacky CHOW, Axel EBELING, and Bill TESKEY, Canada

1. INTRODUCTION

Signalized targets are commonly used in modern day terrestrial laser scanning applications. They are commonly used in static terrestrial laser scanning projects as either tie points for registering multiple point clouds together or as ground control points for georeferencing the point clouds. Although targetless registration techniques, such as the iterative closest point (ICP) are commonly used because it can exploit the vast amount of redundancy in overlapping point clouds to improve the quality of the registration, it has a few major drawbacks. First, georeferencing the point clouds is difficult if not impossible. Second, if insufficient features exist in the overlapping regions (e.g. a flat wall is scanned) ICP has troubles solving for a unique set of transformation parameters. And finally, in certain applications like deformation monitoring, distinct points that are stable or at least with known movements are required to reliably establish the datum between epochs. One of the easiest ways to overcome these issues is by using signalized targets to establish point-to-point correspondence between point clouds. If the scanning is performed outdoors, then the need to perform registration or georeferencing can be completely eliminated by integrating GPS/INS position and orientation information with the laser scanner (e.g. the Riegl VZ400). However, such approaches increase the operational cost significantly if only a small area needs to be scanned and indoor scanning with such system is not yet achievable. But nonetheless, signalized targets can still act as check points for quality control in outdoor direct georeferencing scenarios.

There are currently many different signalized target designs available for laser scanning on the market depending on the manufacturer and model of the laser scanner. Some of the more common designs include planar, spherical, cylindrical, and pyramidal type targets. There are advantages and disadvantages of every design, for example many argue that spherical targets are better than planar targets because the accuracy of target measurement is independent of the incidence angle of the laser, unlike planar targets. However, spherical targets are difficult to be used for georeferencing purposes because the centroid cannot be easily surveyed. Planar targets are still beneficial because they can be manufactured at a lower cost than all the other target designs. In addition, it can be used for both registration of point clouds and georeferencing. Although hemispherical targets do exist which allows the centroid of the sphere to be surveyed accurately from one side of the target, it is expensive to manufacture and calibrate these targets. Among the various designs of laser scanner targets, only the simplest design, planar targets are studied in this paper.

This paper begins by describing the design of the low cost planar targets used for this project. Then a detailed description of the data acquisition process by the Trimble GX terrestrial laser scanner and the Leica TCA2003 high-precision total station is presented. This is followed by

an explanation of the four different methods for measuring the 3D position of the target centroid. The first two methods jointly referred to as the "simplified methods" compute the 3D target coordinates as the mean and median of the irregularly distributed cluster of points captured by the laser scanner. The latter two methods jointly referred to as the "advanced methods" combine the result from least squares plane fitting and circle fitting to compute the 3D coordinate of the target. Finally, the 3D coordinates of 40 targets computed using each of the four methods are compared quantitatively to evaluate both the precision and accuracy under different spatial point density.

2. EXPERIMENT DESCRIPTION

2.1 Target Description

The planar targets are constructed using 8½ by 11 inches Canadian letter size plain white consumer grade paper. A pure black background is printed on every sheet of paper, while exposing a 7.5 centimetre radius circle centered in the middle of the sheet of paper. To allow the targets to be surveyed with a total station, two narrow lines, one horizontal and one vertical, which intersects at the centroid of the circle are also printed. Figure 1 illustrates the design of the target and its appearance in the laboratory.

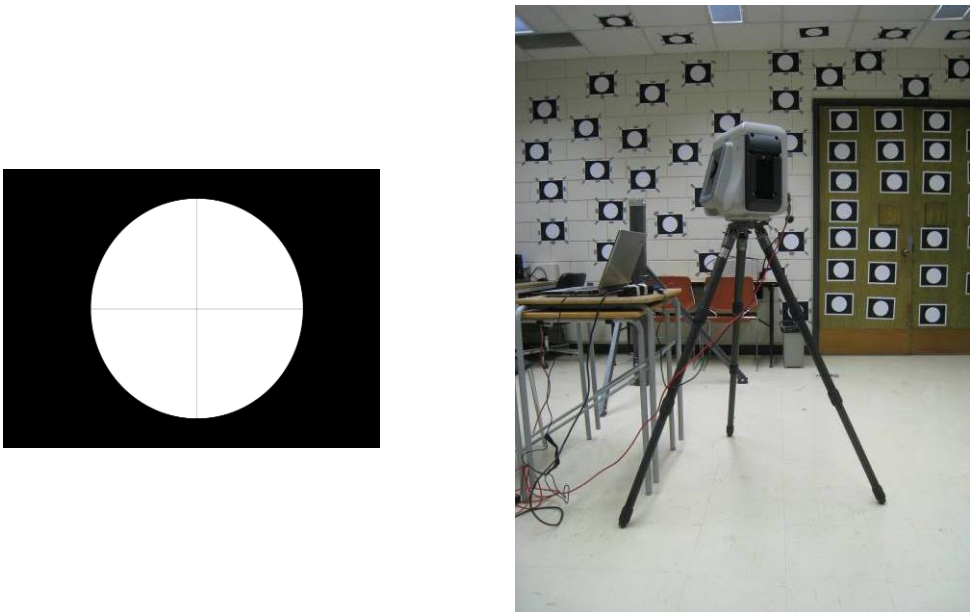

Figure 1: (Left) planar target design used in this project. (Right) digital image of the planar targets used in data collection.

2.2 Laser Scanner Data Acquisition

A total of 40 targets distributed on four different walls in a 5m by 5m by 3m laboratory (Figure 2) were scanned using the latest Trimble pulse-based terrestrial laser scanner, the Trimble GX. The GX is a hybrid scanner with a horizontal field of view of 360^o and a vertical field of view ranging from -20^o to +40^o. This is an active sensor that observes 3D

object space coordinates, as well as intensity information, and 8 bit RGB colour information for every point. It can scan at a rate up to 5000 points per second and has a built-in dual-axis compensator, which was activated during the duration of the data capture. The laser scanner was setup approximately in the centre of the laboratory and all 40 targets were observed with a spatial point density of 2mm or better in a single 360^{o} scan. Two distance measurements were made to every observed point and averaged to reduce the effect caused by the range jitter. Atmospheric correction has been applied to all the range measurements. The temperature, pressure, and humidity were controlled and remained stable during the data collection campaign. To reduce the vibration effect in all measurements a heavy duty camera tripod designed for indoor scanning was used (Figure 1) to eliminate the need for tripods setup on spiders, which can be quite unstable for an indoor environment.

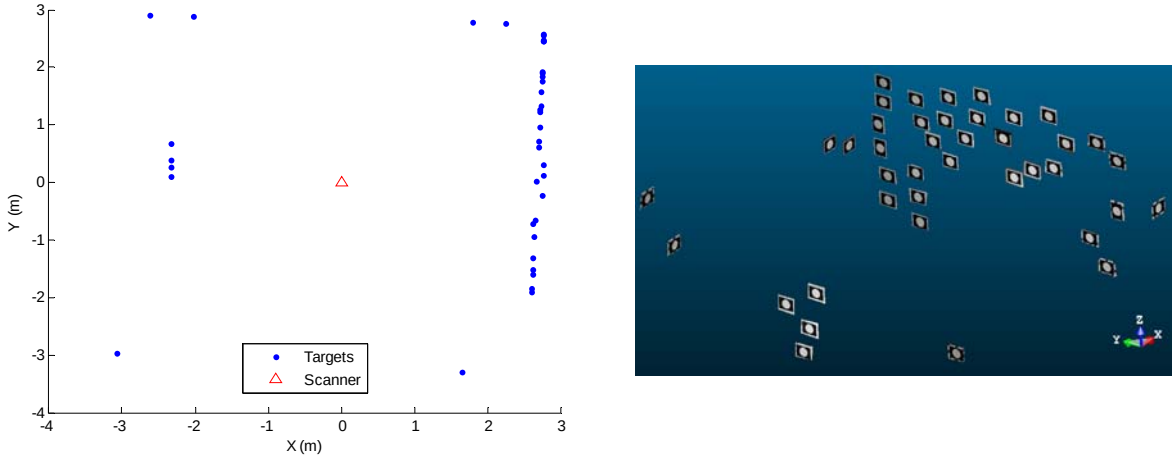

Figure 2: (Left) Top view of the target distribution. (Right) 3D view of the target distribution in the collected laser scanner point cloud.

2.3 Total Station Data Acquisition

A Leica TCA2003 high-precision total station was used for establishing accurate 3D object space coordinates for all the targets. According to the manufacturer, this instrument has an angular measurement accuracy of 0.5 arcsecond and a distance measurement accuracy of 1mm+1ppm. These coordinates will act as check points later on for determining the accuracy of each laser scanner target measurement method. The total station was set up on two stable pillars securely mounted onto the floor and manufactured from structural steel (Figure 3). This was done to ensure the maximum stability of the station setup during data capture. Observations include horizontal directions, zenith angles and slope distances to all 40 targets. The targets were surveyed in two rounds of direct and reverse readings from both pillars with the distance to every target measured with the help of a calibrated peanut prism.

Figure 3: 2D image of the total station setup

3. DATA PROCESSING

3.1 Laser Scanner Target Measurement

All four target measurement algorithms can be generalized into two major tasks: segmentation followed by target centroid measurement. The segmentation process is the same for all methodologies and is explained in the following subsection. The centroid measurement procedure is fairly different between the simplified methods and the advanced methods, and will be explained in sections 3.1.2 and 3.1.3, respectively.

3.1.1 Segmentation

Regardless of the target measurement algorithm, the white circle needs to be separated from the background (Figure 1). This is accomplished by exploiting the fact that the target has a discreet change in gray values between the circle and the background. Laser scanner measurements made on the white circle have a significantly larger intensity value than the black background because of the difference in albedo. This difference in object reflectivity made segmentation by a simple intensity threshold possible. For the dataset gathered, an intensity threshold of 70 was chosen after studying the data's intensity histogram. Figure 4 shows one of the signalized targets segmented into two regions based on the intensity. A similar intensity segmentation approach was applied to other datasets captured by the GX and an older laser scanner, the Trimble (formerly known as Mensi) GS200, and proves to be effective for segmenting the signalized targets.

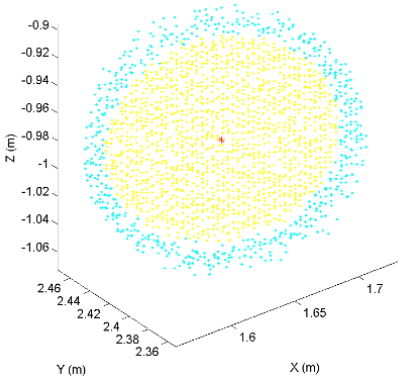

Figure 4: A sample segmented target. Yellow indicates regions with an intensity larger than 70 and cyan indicates regions with an intensity less than or equal to 70.

3.1.2 Simplified Methods

The simplified methods are based solely on computations carried out on the extracted circle. From the 3D object space coordinates of the circle a simple mean and median calculation is performed. Both the mean and median X, Y, Z Cartesian coordinates would represent the 3D centroid of the cluster of points, which is equivalent to the centre of the target. Theoretically, both the mean and median should provide a very similar solution given a large number of points. But if outliers exist in the dataset then the mean would be biased because it is known to be more vulnerable to the presence of blunders when compared to the median (González et al., 2008).

3.1.3 Advanced Methods

The two advanced methods explained in this paper are the same, with the exception of the edge detection algorithm. The advanced methods perform plane fitting and circle fitting as a two step process rather than as a circle fitting in 3D as described in Bayly and Teskey (1992). This is done because of the need to perform edge detection, which can be simplified significantly if performed in 2D. Both methods begin by fitting a plane through the point cloud belonging to a target while minimizing the normal distances between the plane and all the points using a Gauss-Helmert least-squares adjustment model. The functional model used to accomplish this is shown in Equation 1, where $\begin{bmatrix} a & b & c \end{bmatrix}$ are the components of the plane's normal vector and d is the shortest distance between the plane and the origin.

$$aX + bY + cZ - d = 0 \qquad \text{Equation 1}$$

Once the best fit plane is determined, the normal vector of the plane (i.e. a, b, and c) are used to compute the rotation matrix that rotates all the points into the XY-plane. With the normal vector parallel to the Z-axis, the shortest orthogonal distance between the plane and the origin of the laser scanner coordinate system (i.e. d), is the depth of the centroid in this rotated 2D coordinate system denoted as the Z' coordinate. To determine the planimetric coordinates of the centroid in this rotated coordinate system (i.e. X' and Y') the edge points need to be

identified and used as observations for computing the parameters of the best fit circle using the Gauss-Helmert least-squares adjustment model. The main challenge in detecting the edge points in the irregular laser scanner point cloud is that there is no guarantee that a point on the edge has actually been observed.

The first method is based on the method implemented in Lichti et al. (2007). The intensity information from the irregular point cloud is resampled using a bilinear interpolation to generate a 2D intensity image. The Canny edge detector is then used to identify pixels in the image that suggest a significant change in gray value. The X' and Y' coordinates corresponding to these edge pixels are used as the observations in the circle fitting. One of the drawbacks of this approach is that the observations are derived from the interpolated data, however since the targets are planar, using a bilinear interpolation is justifiable.

The second method removes the need to perform interpolation and uses points closest to the edge in both the circle and the background as observations instead. By exploiting the a priori knowledge about the linear scanning pattern and the structure the data was output to file, for every unique increment in the X' direction the point with the maximum and minimum Y' coordinate of that scan line belonging to the circle is extracted. It is important to note that due to random noises in the angular measurements of the laser scanner coupled with the scanner's own vibration during data collection only a significant change in X' coordinate that is larger than the random noise indicates a new scan line. Hence, this algorithm is only feasible if the random noise is low. Once the points closest to the edge in the circle are identified, the points in the background that are closest to these edge points are identified and used as observations as well. Although this method removes the necessity of resampling the data, it suffers from the quantization problem where only a few or none of the observations actually fall on the edge of the circle. Therefore, the position of the best fit circle can only be defined as located between the outer periphery of the circle and the inner limits of the background. Regardless of the edge detection method, once the edge observations are obtained the parameters of the best fit circle are computed using the functional model shown in Equation 2. Where, X' and Y' are the planimetric coordinates of the detected edge in the rotated coordinate system, X_c and Y_c are the centroid coordinates of the best fit circle, and r is the radius of the circle.

$$(X'-X_c)^2+(Y'-Y_c)^2-r^2=0 \qquad \text{Equation 2}$$

The centroid of this best fitting circle is equivalent to the planimetric coordinates of the centroid of the target in this rotated coordinate system. With the planimetric coordinates and depth of the centroid determined, the last step is simply reverse the rotations applied before to rotate coordinates of the centroid back to its original orientation. One other benefit of the advanced methods is that least-squares adjustment is used, so the standard deviation of the centroid can be computed and other typical reliability measures and outlier detection can be implemented (Ghilani et al., 2006).

3.2 Survey Network Adjustment

Observations collected with the total station were first reduced, averaged and screened for outliers. The observed zenith angles and slope distances were converted to corresponding horizontal distances and height differences, which allow for a more linear and thus robust normal equation system. A least-squares adjustment of these observations using the Gauss-Markov model was then performed to obtain 3D object space coordinates and accuracies for the targets. Since all targets were observed from two stations, there is a redundancy of two for the horizontal position of each target. There are two independent observations of the elevation of each target, so the redundancy in the vertical is one. Inner constraints were applied to all 40 target points to define the geodetic datum. After the adjustment, data snooping was performed to ensure that no erroneous observations would affect the solution. Then, variance components were estimated for each observation group so more realistic accuracy estimates could be determined for the target point coordinates from the scaled covariance matrix.

4. QUALITY ASSESSMENT

4.1 Precision (Internal Accuracy)

The four different target centroid measurement algorithms are applied to the original point clouds of the 40 targets with a spatial point density no sparser than 2mm. With this acting as the best estimate of the true coordinates of the centroid, the density of the point clouds of the 40 targets is reduced using Trimble RealWorks Survey 6.0 until the spatial point density is 3mm and then the four target measurement algorithms are applied again. The coordinate differences between the original density and reduced point density are then used for computing the RMS. The same is then repeated for the targets with the spatial point density reduced to 4mm, 5mm, all the way up to 10mm.

The plots in Figure 5 show the change in RMS in the horizontal direction and the vertical direction as a function of change in spatial point density. Note that the RMS in the X and Y directions are combined as the horizontal RMS so that it is independent of the horizontal target distribution relative to the heading of the laser scanner. Also, the RMS in the vertical direction is equivalent to the RMS in the Z direction because during data capture the scanner was leveled.

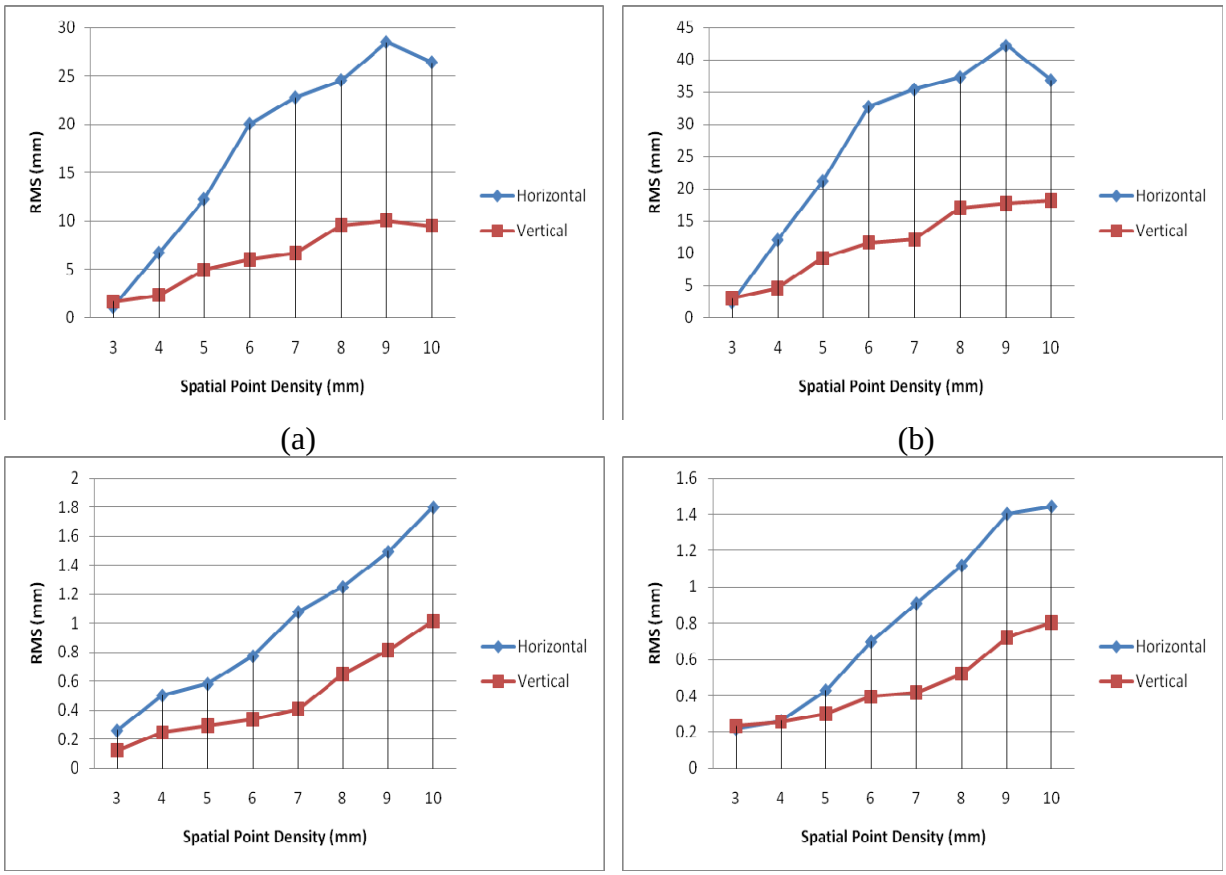

Figure 5: (a) target measurement precision when using the mean. (b) target measurement precision when using the median. (c) target measurement precision when using geometric form fitting and edges detected from the interpolated intensity image. (d) target measurement precision when using geometric form fitting and edges detected from the raw point cloud.

It can be deduced from Figure 5 that at high spatial point density (e.g. 3mm) all four methods produce reasonable precision. The simplified methods measured the centroid with a precision between one to three millimeter, and the advanced method measured with a precision of sub-millimetre. However, as the spatial point density drops the horizontal and vertical centroid coordinates computed as the mean and median begin to change significantly. At a spatial point density of 10mm, because the sample size is so small, the horizontal and vertical RMS is at the centimetre level for the simplified methods. In contrast, the advanced methods appear to be more robust against spatial point density change. At a spatial point density of up to a centimetre, the RMS is still below 1.8mm for the horizontal and 1mm for the vertical. The edge detection algorithm does appear to have a small effect on the precision, the proposed edge detection method that only involves the raw point cloud shows a slightly better precision than the interpolation method combined with the Canny edge detector, but the difference is negligible. It is not unexpected that the advanced methods are more precise, because through the inclusion of geometric form fitting the robustness of the solution is strengthened especially when the spatial point density is low. Three points in 3D space define a plane, and two points in 2D space define a circle if the radius is known a priori. Therefore,

even if the spatial point density is sparse there is still a significant amount of redundancy in the solution to improve not only the precision but also the reliability of the solution in a least-squares adjustment.

Another trend that is noticeable is that the precision in the horizontal is always worse than the vertical regardless of the target measurement algorithm. This is simply due to the fact that at close range the GX has a better angular measurement precision than the range. Also, all the observed planar targets happen to have a normal vector that is orthogonal to the vertical axis. If all the targets observed were on the ceiling or on the floor, the opposite trend would be observed. In addition, if the distance measurements were averaged even more, the horizontal precision would be improved further.

4.2 Accuracy (External Accuracy)

The 3D coordinates from the total station survey network were all well determined with a precision in the sub-millimetre level. To perform the check point analysis they will be treated as the true ground coordinates. A 3D rigid body transformation with the datum defined by all 40 targets using inner constraints was applied to relate the laser scanner coordinate system and the total station coordinate system. Inner constraints were adopted to ensure that the computed RMSE is independent of the points chosen for computing the transformation parameters. Since two different instruments were used for measuring the targets (i.e. laser scanner and total station) intuitively a scale factor should be included in the transformation to relate the two independent datasets. However, it was discovered that the scale difference between the two instruments was statistically insignificant and only short distances were observed. The target centroid measurement accuracy for all four algorithms expressed in terms of RMSE is graphically presented in Figure 6.

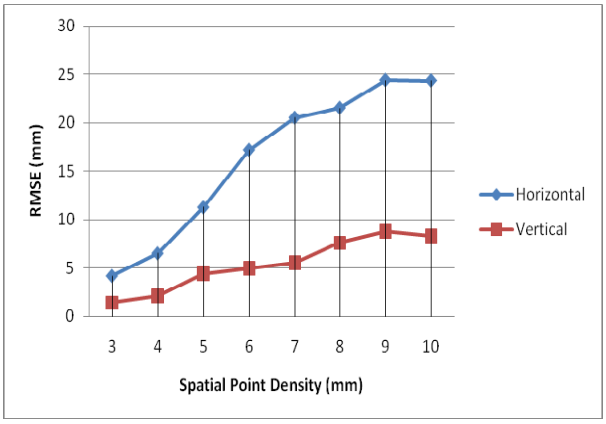

(a)

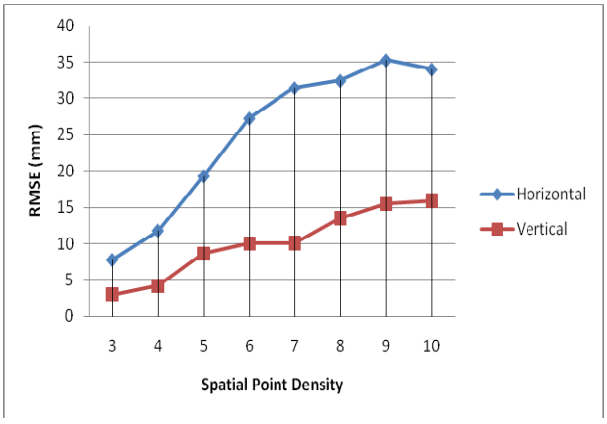

(b)

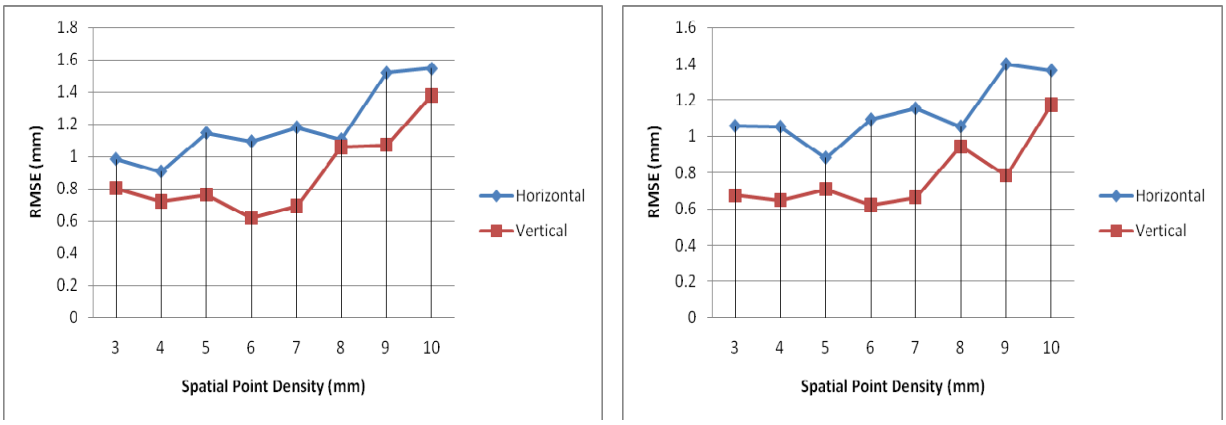

(c) (d)

Figure 6: (a) target measurement accuracy when using the mean. (b) target measurement accuracy when using the median. (c) target measurement accuracy when using geometric form fitting and edges detected from the interpolated intensity image. (d) target measurement accuracy when using geometric form fitting and edges detected from the raw point cloud.

The RMSE for the four algorithms follow a very similar trend as the RMS plots shown in Figure 5 and exhibit similar magnitudes of errors. The simplified methods are more sensitive to the spatial point density and are less accurate than the advanced methods. There is not a significant difference in RMSE between Figure 6 (c) and Figure 6 (d) to suggest that one edge detection algorithm is superior compared to the other. Nonetheless, using either advanced methods, sub-millimetre level target measurement accuracy is achievable even with targets constructed from consumer grade paper.

To improve the accuracy of the target centroid measurement, either a higher spatial point density or a larger target could be used. Both would result in an increase in the observational redundancy and higher probability of a single point measurement landing on the edge of the circle. Other improvement possibilities that may be instrument dependent include: averaging the distance measurements, averaging the angular measurements, and reducing the size of the footprint at the target distance.

5. CONCLUSIONS

This paper presented a precision and accuracy comparison of four potential methods for measuring the centroid of a planar target. The experiment conducted utilized only targets made from regular paper and demonstrated that sub-millimeter level precision and accuracy is achievable for a laboratory environment using the advanced methods. The advanced methods are superior to the simplified methods in terms of precision, accuracy, and robustness. It has been proven that by incorporating geometric form fitting to target centroid measurement the precision, accuracy, and reliability of the measurement can be improved. Furthermore, it can also provide a variance-covariance matrix of the centroid coordinates because least-squares adjustment is adopted. All methods presented are instrument independent with the flexibility of having the target printed with different sizes, which may be beneficial for outdoor scanning projects over long distances.

REFERENCES

Bayly, D. A., & Teskey, W. F. (1992). Close-range High-precision Surveys for Machinery Alignment. *CISM Journal ACSGC, 46(4)* , 409-421.

Ghilani, C., & Wolf, P. (2006). *Adjustment Computations Spatial Data Anaylsis.* New Jersey: John Wiley & Sons, Inc.

González, R., & Woods, R. (2008). *Digital Image Processing.* New Jersey: Prentice Hall, 2008.

Lichti, D., Brustle, S., & Franke, J. (2007). Self-calibration and analysis of the Surphaser 25HS 3D scanner. *Strategic Integration of Surveying Services, FIG Working Week 2007* (s. 13). Hong Kong SAR, China: May 13-17, 2007.

BIOGRAPHICAL NOTES

Jacky Chow is currently a full-time graduate student in Geomatics Engineering at the University of Calgary. His research focuses on high-precision deformation monitoring and 3D imaging, in particular terrestrial laser scanning. His research interests include sensor calibration, point cloud classification, automatic surface matching, and more.

Axel Ebeling received his diploma in Surveying Engineering from the Technical University of Berlin, Germany in 2006. He is currently enrolled in a PhD program in the Department of Geomatics Engineering at the University of Calgary. He is Project Manager in the "Intelligent Structural Monitoring" NSERC CRD Project. His research work focuses on the application of least-squares to high-precision surveys, especially to deformation monitoring.

Bill Teskey is a Professor in the Department of Geomatics Engineering at the University of Calgary. He is a registered Professional Engineer in Alberta and a registered Land Surveyor in Alberta and Canada. Bill served for a number of years on the Western Canadian Board of Examiners for Land Surveyors and on the Board of Examiners of the Association of Professional Engineers, Geologists and Geophysicists of Alberta. His areas of interest are precise engineering and deformation surveys. He is currently Principal Investigator in the "Intelligent Structural Monitoring" NSERC CRD Project.

CONTACTS

Jacky Chow
Department of Geomatics Engineering
Schulich School of Engineering, University of Calgary
2500 University Drive N.W.
Calgary, Alberta, T2N 1N4
Canada
Tel. +1 (403) 220-3582
Fax + 1 (403) 284-1980
Email: jckchow@ucalgary.ca

Axel Ebeling
Department of Geomatics Engineering
Schulich School of Engineering, University of Calgary
2500 University Drive N.W.
Calgary, Alberta, T2N 1N4
Canada
Tel. +1 (403) 220-4565
Fax + 1 (403) 284-1980
Email: aebeling@ucalgary.ca

Prof. Dr. Bill Teskey
Department of Geomatics Engineering
Schulich School of Engineering, University of Calgary
2500 University Drive N.W.
Calgary, Alberta, T2N 1N4
Canada
Tel. +1 (403) 220-7397
Fax + 1 (403) 284-1980
Email: wteskey@ucalgary.ca